Structural damage assessment using linear approximation with maximum entropy and transmissibility data

V. Meruane[a], A.Ortiz-Bernardin[a]

[a]*Department of Mechanical Engineering, Universidad de Chile, Beauchef 850, Santiago, Chile*

Abstract

Supervised learning algorithms have been proposed as a suitable alternative to model updating methods in structural damage assessment, being Artificial Neural Networks the most frequently used. Notwithstanding, the slow learning speed and the large number of parameters that need to be tuned within the training stage have been a major bottleneck in their application. This article presents a new algorithm for real-time damage assessment that uses a linear approximation method in conjunction with antiresonant frequencies that are identified from transmissibility functions. The linear approximation is handled by a statistical inference model based on the maximum-entropy principle. The merits of this new approach are twofold: training is avoided and data is processed in a period of time that is comparable to the one of Neural Networks. The performance of the proposed methodology is validated by considering three experimental structures: an eight-degree-of-freedom (DOF) mass-spring system, a beam, and an exhaust system of a car. To demonstrate

Email addresses: vmeruane@ing.uchile.cl (V. Meruane), aortizb@ing.uchile.cl (A.Ortiz-Bernardin)

the potential of the proposed algorithm over existing ones, the obtained results are compared with those of a model updating method based on parallel genetic algorithms and a multilayer feedforward neural network approach.

Keywords: Structural damage assessment, supervised learning algorithms, maximum-entropy principle, linear approximation

---

1. Introduction

The purpose of structural damage assessment is to detect and characterize damage at the earliest posible stage, and to estimate how much time remains before maintenance is required, the structure fails or the structure is no longer functional. Damage assessment has a tremendous potential for life-safety and/or economic benefits, this generates a wide interest in the civil, mechanical and aerospace engineering fields.

A global technique called vibration-based damage assessment [1] has been rapidly expanding over the last few years. The basic idea is that vibration characteristics (natural frequencies, mode shapes, damping, frequency response function, etc) are functions of the physical properties of the structure. Thus, changes to the material and/or geometric properties due to damage will cause detectable changes in the vibrations characteristics. Many studies have demonstrated that vibration measurements are sensitive enough to detect damage even if it is located in hidden or internal areas [2].

Vibration-based damage assessment methods are classified as model-based or non-model based. Non-model-based methods detect damage by comparing the measurements from the undamaged and damaged structures, whereas model-based methods locate and quantify damage by correlating an analyt-

ical model with test data from the damaged structure. Non-model-based methods usually provide the first two levels of damage assessment (detection and location), whereas model-based methods can achieve up to the third level (quantification). Additionally, model-based methods are particularly useful for predicting the system response to new loading conditions and/or new system configurations (damage states), allowing damage prognosis [3].

Model-based damage assessment requires the solution of a nonlinear inverse problem, which can be accomplished using supervised learning algorithms as neural networks or by global optimization algorithms. The most successful applications are model updating methods based on global optimization algorithms [4, 5, 6, 7, 8]. Model updating is an inverse method that identifies the uncertain parameters in a numerical model and is commonly formulated as an inverse optimization problem. In model updating-based damage assessment, the algorithm uses the differences between the models of the structure that are updated before and after the presence of damage to localize and determine the extent of damage. The basic assumption is that the damage can be directly related to a decrease of stiffness in the structure. However, these algorithms are exceedingly slow and the damage assessment process is achieved via a costly and time-consuming inverse process, which presents an obstacle for real-time damage assessment applications. Real-time damage assessment allows to continuously monitor the state of a structure, which is critical to avoid catastrophic failures. For example, many catastrophic collapses of wind turbines could have been avoided if the damage had been detected and the turbines had been stopped in time [9].

To reduce the time required to assess damage, supervised learning algo-

rithms have been proposed as an alternative to model updating. The objective of supervised learning is to estimate the structure's health based on current and past samples. Supervised learning can be divided into two classes: parametric and non-parametric. Parametric approaches assumed a statistical model for the data samples. A popular parametric approach is to model each class density as Gaussian [10]. Nonparametric algorithms do not assume a structure for the data. The most frequently nonparametric algorithms used in damage assessment are Artificial Neural Networks [11, 12, 13, 14]. A trained neural network can potentially detect, locate and quantify structural damage in a short period of time. Hence, it can be used for real-time damage assessment.

There are different types of network architectures, among which multilayer feedforward networks are the most frequently used. Although once the network is already trained it can process data very quickly, the slow learning speed and the large number of parameters that need to be tuned within the training stage have been a major bottleneck in their application [14]. Gupta et al. [15, 16] presented a new nonparametric method, which generalizes linear approximation by using the maximum-entropy (max-ent) principle [17] for statistical inference. A similar approach is adopted by Erkan [18] for semi-supervised learning problems, where a decision rule is to be learned from labeled and unlabeled data. Recently, max-ent methods have become quite popular in the computational mechanics community as a powerful tool for numerical solution of PDEs [19, 20], and their applications in the solution of ill-posed inverse problems have also been explored, which includes damage assessment applications [21, 22]. By using max-ent linear approximation

methods, training is avoided and data is processed in a period of time that is comparable to the one of Neural Networks. In addition, it only requires one parameter to be selected. Hence, max-ent linear approximation methods become very appealing for real-time health monitoring applications. Gupta [15] demonstrated the application of the max-ent linear approximation approach to color management and gas pipeline integrity problems. In the present paper, we demonstrate the applicability in structural damage identification.

An important aspect of structural damage assessment is the selection of an appropriate measure of the system response. The idea of using directly the frequency response functions (FRFs) has attracted many researchers [23]. Among all the dynamic responses, the FRF is one of the easiest to obtain in real-time, as the *in situ* measurement is straightforward. Nevertheless, FRFs have the disadvantage that they cannot be identified from output-only modal analysis; thus the measurement of the excitation force is always required. For structures in real conditions, it often becomes very difficult to measure the excitation force. Thus, a critical issue is to reduce the dependence upon measurable excitation forces. An alternative to FRFs are transmissibility functions. They relate the responses at two sets of co-ordinates. Consequently, they do not involve the measurement of excitation forces. The only condition is that the location of the excitation force must be known.

The majority of the research in transmissibility-based damage identification are data-based approaches for damage detection and localization. Chesné and Deraemaeker [24] presented a review of them, in addition to a study of the feasibility of transmissibility functions for damage detection and localization. The researchers concluded that extreme care should be

taken when using transmissibility functions in an unsupervised manner, i.e. without knowing how they will be affected by damage, because damage localization is not always guaranteed. The first study of transmissibility functions as indicators of structural damage was presented by Worden [25]. The researcher showed for a simple lumped-parameter system that transmissibilities are able to detect small stiffness changes. Since then, the research group leaded by Worden and Manson have done extensive research in this topic [26]. In [27], the researchers used a representative aircraft skin panel to investigate the sensitivity of transmissibility features to damage. Damage detection is achieved via a statistical outlier analysis. This algorithm was later compared with the performance of density estimations and auto-associative neural networks in [28]. The feature vector was constructed from transmissibility data, selecting spectral lines centered at a particular peak and then using PCA to reduce the dimension of the data set. Outlier analysis and neural networks prove to be more sensitive to damage. Manson et al. [29, 30] tested the performance of the outlier analysis technique to detect damage in an inspection panel of a Gnat aircraft. Damage was introduced as holes and saw-cuts across the panel. To achieve the next step of damage assessment, i.e. localization, Pierce et al. [31] proposed an interval-based classification network. Experimental transmissibility data was collected from a series of undamaged and damaged scenarios. The performance of the network was evaluated with unseen test data, obtaining a classification rate of 91%. Around the same time as Worden, Zhang et al. [32] presented a methodology to detect experimental damage using changes in the transmissibility functions. Transmissibility functions were derived from structural translations and from curvatures, be-

ing the last ones the most sensitive to damage. Johnson and Adams [33] have also studied the use of transmissibility functions for detecting, locating and quantifying damage. They demonstrated that since transmissibility functions are determined solely by the system zeroes (antiresonant frequencies), they are potentially better indicators of localized damage. These results were used to develop a framework for transmissibility-based damage identification using smart sensor arrays [34]. The damage feature is constructed based on the changes of the logarithms of transmissibility functions due to damage. Maia et al. [35] presented a method for computing the transmissibility matrix from responses only. They showed that transmissibility functions are sensitive to damage making them a possible approach for damage assessment. A similar approach was used to explore the ability of a transmissibility method for detecting and localizing damage [36]. The researchers concluded that it is possible to detect sensitive changes to damage but further research is needed. In a later work, Maia et al. [37] compared two damage indicators constructed with transmissibly functions and with frequency response functions. They concluded that the method based on transmissibility measurements is much more sensitive for the detection and relative quantification of damage.

Transmissibility functions have also been used in model updating. Steenackers et al. [38] proposed to use transmissibility measurements instead of frequency response functions in model updating. The researchers updated the finite element model of a mobile substation support structure using driving point transmissibility poles. Driving point transmissibility poles correspond to the resonances of the structure when the excitation degree of freedom is constrained. This is equivalent to the antiresonant frequencies of the driving

point frequency response function. The authors concluded that the finite element model updated with transmissibility information is equivalent to the model updated with FRFs or operational modes. Hence, transmissibility functions are a good alternative in model updating when the excitation force is not measured. Meruane [39] presented a model updating and damage assessment algorithm that uses antiresonant frequencies derived from transmissibility data. Antiresonance frequencies correspond to the dips in FRFs and consequently to the dips and peaks in transmissibility functions. Hence, it is possible to identify antiresonance frequencies using transmissibility information. Transmissibility functions seem to be quite promising in diverse fields such as output-only modal analysis [40, 41, 42], model updating and damage assessment.

The primary contribution of this research is the development of a novel real-time damage assessment algorithm that uses a linear approximation method in conjunction with antiresonant frequencies that are identified from transmissibility functions. The linear approximation is handled by a statistical inference model based on the maximum-entropy principle [17]. The merits of this new approach are twofold: training is avoided and data is processed in a period of time that is comparable to the one of Neural Networks. The performance of the proposed methodology is validated by considering three experimental structures: an eight-degree-of-freedom (DOF) mass-spring system, a beam, and an exhaust system of a car. To demonstrate the potential of the max-ent linear approximation method over existing ones, results obtained via the max-ent formalism are compared with those of a model updating method based on parallel genetic algorithms [39] and a multilayer

feedforward neural network approach [14].

The remainder of this work is structured as follows: Section 2 provides general antecedents and related research on the max-ent linear approximation method. Section 3 describes the setting up of the database. Sections 4 presents the case studies and the damage assessment results using three approaches: feedforward neural networks, model updating with parallel genetic algorithms and max-ent linear approximation. Finally, conclusions and forthcoming work are presented in Section 5.

2. Linear approximation with maximum-entropy principle

The main problem of vibration-based damage assessment is to ascertain the presence, location and severity of structural damage given a structure's dynamic characteristics. This principle is illustrated in Fig. 1; the vibration characteristics of the structure, which in this case correspond to antiresonant frequencies, act as the input to the algorithm, and the outputs are the damage indices of each element in the structure.

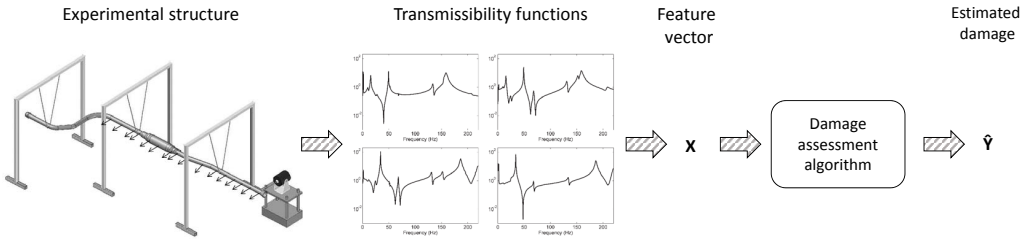

Figure 1: Scheme of the damage assessment algorithm.

Let the observation vector $\mathbf{Y}^j = \left\{Y_1^j, Y_2^j, \ldots, Y_m^j\right\} \in \mathbb{R}^m$ represents the jth damage state of a structure, where m is the number of structural ele-

ments. Let the feature vector $\mathbf{X}^j = \left\{X_1^j, X_2^j, \ldots, X_n^j\right\} \in \mathbb{R}^n$ represent a set of characteristics parameters of the structure (antiresonant frequencies) associated to the damage state $\mathbf{Y}^j$. The variables $\mathbf{X}$ and $\mathbf{Y}$ have joint distribution $P_{X,Y}$. A set of k independent and identically distributed samples be drawn from $P_{X,Y}$, these samples represent the database $(\mathbf{X}^1, \mathbf{Y}^1), (\mathbf{X}^2, \mathbf{Y}^2), ..., (\mathbf{X}^k, \mathbf{Y}^k)$. The central problem in supervised learning is to form an estimate of $P_{Y|X}$, i.e. given a certain feature $\mathbf{X}$ to estimate the corresponding observation $\mathbf{Y}$. Let $\hat{\mathbf{Y}}$ denote the estimated value of $\mathbf{Y}$. Linear approximation takes the N nearest neighbors to a test point $\mathbf{X}$ and uses a linear combination of them to represent $\mathbf{X}$ as

$$\mathbf{X} = \sum_{j=1}^{N} w_j(\mathbf{X})\mathbf{X}^j(\mathbf{X}), \quad \sum_{j=1}^{N} w_j(\mathbf{X}) = 1, \tag{1}$$

where $w_1, w_2, \ldots, w_N$ are weighting functions, and $\mathbf{X}^1(\mathbf{X}), \mathbf{X}^2(\mathbf{X}), \ldots, \mathbf{X}^N(\mathbf{X})$ are the N closest neighbors to a test point $\mathbf{X}$ out of the database set. The equations given in (1) can be expressed as the following system of linear equations:

$$\mathbf{A}\mathbf{w} = \mathbf{b}, \tag{2}$$

$$\text{with } \mathbf{A} = \begin{bmatrix} X_1^1 & X_1^2 & \ldots & X_1^N \\ X_2^1 & X_2^2 & \ldots & X_2^N \\ \vdots & \vdots & \ddots & \vdots \\ X_n^1 & X_n^2 & \ldots & X_n^N \\ 1 & 1 & \ldots & 1 \end{bmatrix}_{(n+1)\times N}, \ \mathbf{b} = \begin{bmatrix} X_1 \\ X_2 \\ \vdots \\ X_n \\ 1 \end{bmatrix}_{(n+1)\times 1}, \ \mathbf{w} = \begin{bmatrix} w_1 \\ w_2 \\ \vdots \\ w_N \end{bmatrix}_{N\times 1}$$

After $\mathbf{w}$ is obtained from (2), $\hat{\mathbf{Y}}$ is estimated as

$$\hat{\mathbf{Y}} = \sum_{j=1}^{N} w_j(\mathbf{X})\mathbf{Y}^j(\mathbf{X}), \tag{3}$$

where $\mathbf{Y}^1(\mathbf{X}), \mathbf{Y}^2(\mathbf{X}), \ldots, \mathbf{Y}^N(\mathbf{X})$ are the corresponding observations to the N selected neighbors. To solve the linear system given in (2), the number of unknowns N must equal the number of constraints $n+1$. Often there are more than $n+1$ samples that are relevant to estimate a test point $\mathbf{X}$ ($N > n+1$). Thus, the system of linear equations becomes undetermined. The system (2) is very common in computational mechanics (see for instance, [19]) to construct basis functions for approximation of field variables in Partial Differential Equations (PDEs) and for curve and surface fitting in computational geometry (see for instance, [43]). Typically, when (2) is undetermined, its solution is tackled via an unconstrained optimization technique of the family of least-squares. However, these methods produce some negative weights, which lacks physical meaning. An alternative that produces positive weights is obtained via the maximum-entropy (max-ent) variational principle [17].

The notion of entropy in information theory was introduced by Shannon as a measure of uncertainity [44]. Later, on using the Shannon entropy, Jaynes [17] postulated the maximum-entropy principle as a rationale means for least-biased statistical inference when insufficient information is available. The maximum-entropy principle is suitable to find the least-biased probability distribution when there are fewer constraints than unknowns and is posed as follows:

Consider a set of N discrete events $\{x_1, \ldots, x_N\}$. The possibility of each

event is $p_i = p(x_i) \in [0,1]$ with uncertainty $-\ln p_i$. The Shannon entropy $H(\mathbf{p}) = -\sum_{i=1}^{N} p_i \ln p_i$ is the amount of uncertainty represented by the distribution $\{p_1, \ldots, p_N\}$. The least-biased probability distribution and the one that has the most likelihood to occur is obtained via the solution of the following optimization problem (maximum-entropy principle):

$$\max_{\mathbf{p}\in\mathbb{R}_+^N} \left[H(\mathbf{p}) = -\sum_{i=1}^{N} p_i \ln(p_i) \right], \tag{4a}$$

subject to the constraints:

$$\sum_{i=1}^{N} p_i = 1, \quad \sum_{i=1}^{N} p_i g_r(x_i) =< g_r(x) >, \tag{4b}$$

where $\mathbb{R}_+^N$ is the non-negative orthant and $< g_r(x) >$ is the known expected value of functions $g_r(x)$ $(r = 0, 1, \ldots, m)$, with $g_0(x) = 1$ being the normalizing condition.

The optimization problem (4) assigns probabilities to every x_i in the set. Now, assume that the probability p_i has an initial guess m_i known as a *prior*, which reduces its uncertainty to $-\ln p_i + \ln m_i = -\ln(p_i/m_i)$. An alternative problem can be formulated by using this *prior* in (4) [45]:

$$\max_{\mathbf{p}\in\mathbb{R}_+^n} \left[H(\mathbf{p}) = -\sum_{i=1}^{N} p_i \ln\left(\frac{p_i}{m_i}\right) \right], \tag{5a}$$

subject to the constraints:

$$\sum_{i=1}^{n} p_i = 1, \quad \sum_{i=1}^{n} p_i g_r(x_i) =< g_r(x) > . \tag{5b}$$

In (5), the variational principle associated with $\sum_{i=1}^{N} p_i \ln\left(\frac{p_i}{m_i}\right)$ is known as *the principle of minimum relative (cross) entropy* [46, 47]. Depending upon the *prior* employed, the optimization problem (5) will favor some x_i in the set by assigning more probability to them, and eventually, assigning non-zero probability ($p_i > 0$) to a selected number of x_i ($i < N$) in the set. It can be easily seen that if the *prior* is constant, the Shannon-Jaynes entropy functional (4) is recovered as a particular case. The max-ent approach is demonstrated next by means of two dice experiments.

Example 2.1. *A fair dice is thrown. The set of possible outcomes are the events* $\{1, 2, 3, 4, 5, 6\}$. *Since the dice is fair, we infer that all the events have equal possibility* $1/6$ *of being the outcome. Taking the expectation of the outcome yields:*

$$E = \frac{1}{6} \cdot 1 + \frac{1}{6} \cdot 2 + \frac{1}{6} \cdot 3 + \frac{1}{6} \cdot 4 + \frac{1}{6} \cdot 5 + \frac{1}{6} \cdot 6 = 3.5.$$

If this expectation is viewed as the constraint in the max-ent problem (4), the set of possibilities previously inferred is exactly predicted by max-ent. The result is shown in Fig. 2.

Example 2.2. *A biased dice is thrown. The set of possible outcomes are the events* $\{1, 2, 3, 4, 5, 6\}$. *A guess is made on each outcome via the following set of prior possibilities* $w = \{0.1, 0.1, 0.1, 0.1, 0.5, 0.1\}$. *On considering these priors, the expectation of the outcome yields:*

$$E = 0.1 \cdot 1 + 0.1 \cdot 2 + 0.1 \cdot 3 + 0.1 \cdot 4 + 0.5 \cdot 5 + 0.1 \cdot 6 = 4.1.$$

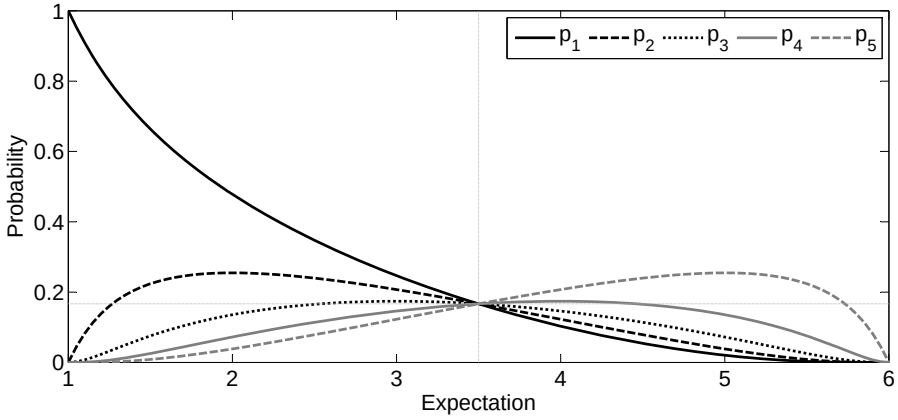

Figure 2: Throwing a fair dice. If the dice is fair, max-ent assigns equal possibilities to all events.

If this expectation is viewed as the constraint in the max-ent problem (5), the set of 'most honest' possibilities assigned by max-ent is $p = \{0.1, 0.1, 0.1, 0.1, 0.5, 0.1\}$*, which is exactly the guess, as expected. The result is depicted in Fig. 3.*

Because of its general character and flexibility, we adopt the relative entropy approach for our problem, where the probability p_i is replaced with the weighting function w_i of the linear approximation problem posed in (1). This reads:

$$\max_{\mathbf{w}\in\mathbb{R}_+^N} \left[H(\mathbf{w}) = -\sum_{i=1}^{N} w_i(\mathbf{X}) \ln\left(\frac{w_i(\mathbf{X})}{m_i(\mathbf{X})}\right) \right], \tag{6a}$$

subject to the constraints:

$$\sum_{i=1}^{N} w_i(\mathbf{X})\tilde{\mathbf{X}}^i = 0, \quad \sum_{i=1}^{N} w_i(\mathbf{X}) = 1, \tag{6b}$$

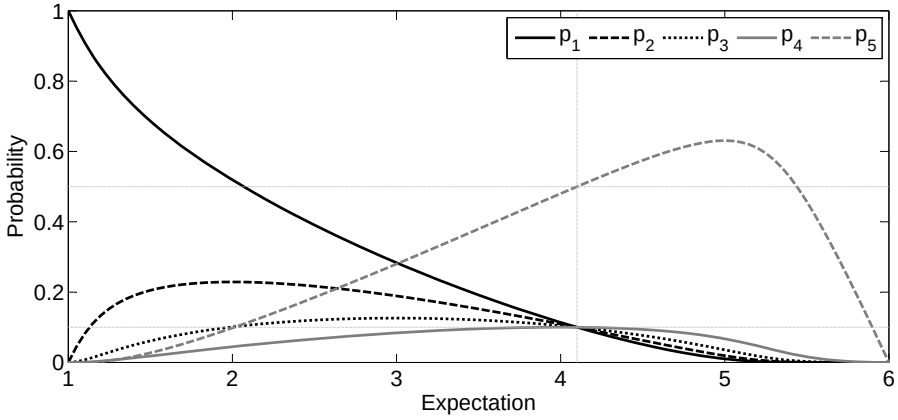

Figure 3: Throwing a biased dice. If the dice is biased, max-ent assigns the most probable possibility to each event.

where $\tilde{\mathbf{X}}^i = \mathbf{X}^i - \mathbf{X}$ has been introduced as a shifted measure for stability purposes. A typical prior distribution is the smooth Gaussian [48]

$$m_i(\mathbf{X}) = \exp(-\beta_i \|\tilde{\mathbf{X}}^i\|^2), \tag{7}$$

where $\beta_i = \gamma / h_i^2$; γ is a parameter that controls the radius of the Gaussian prior at $\mathbf{X}^i$, and therefore its associated weight function; and h_i is a characteristic $n-$dimensional Euclidean distance between neighbors that can be distinct for each $\mathbf{X}^i$. In view of the optimization problem posed in (6) for supervised learning, maximizing the entropy chooses the weight solution that commits the least to any one in the database samples [16].

The solution of the max-ent optimization problem is handled by using the procedure of Lagrange multipliers, which yields [45]:

$$w_i(\mathbf{X}) = \frac{Z_i(\mathbf{X}; \boldsymbol{\lambda}^*)}{Z(\mathbf{X}; \boldsymbol{\lambda}^*)}, \quad Z_i(\mathbf{X}; \boldsymbol{\lambda}^*) = m_i(\mathbf{X}) \exp(-\boldsymbol{\lambda}^* \cdot \tilde{\mathbf{X}}^i), \tag{8}$$

where $Z(\mathbf{X}; \boldsymbol{\lambda}^*) = \sum_j Z_j(\mathbf{X}; \boldsymbol{\lambda}^*)$, $\tilde{\mathbf{X}}^i = [\tilde{X}_1^i \dots \tilde{X}_N^i]^{\mathrm{T}}$ and $\boldsymbol{\lambda}^* = [\lambda_1^* \dots \lambda_N^*]^{\mathrm{T}}$.

In (8), the Lagrange multiplier vector $\boldsymbol{\lambda}^*$ is the minimizer of the dual optimization problem posed in (6) [45]:

$$\boldsymbol{\lambda}^* = \arg \min_{\boldsymbol{\lambda} \in \mathbb{R}^N} \ln Z(\mathbf{X}; \boldsymbol{\lambda}), \tag{9}$$

which gives rise to the following system of nonlinear equations:

$$\mathbf{f}(\boldsymbol{\lambda}) = \nabla_{\boldsymbol{\lambda}} \ln Z(\boldsymbol{\lambda}) = -\sum_{i}^{N} w_i(\mathbf{X}) \tilde{\mathbf{X}}^i = \mathbf{0}, \tag{10}$$

where $\nabla_{\boldsymbol{\lambda}}$ stands for the gradient with respect to $\boldsymbol{\lambda}$. Once the converged $\boldsymbol{\lambda}^*$ is found, the weight functions are computed from (8).

3. Construction of the database

Database samples are generated using a numerical (finite element) model of the structure. Two approaches are used to overcome the dependency on the accuracy of the numerical model. The first is to update the numerical model using experimental data from the undamaged structure. The numerical models corresponding to the three case studies were updated using the algorithm described in [39]. The second is to define an input parameter that considers the initial errors in the numerical model, thus avoiding the need for an accurate numerical model. This goal is achieved using the changes in the data instead of their absolute values [49]. With the validated numerical model, the database is built as follows:

1. Define a set of damage scenarios to be used in the database.
2. Set $j = 1$.
3. Parameterize the jth scenario with an observation vector $\mathbf{Y}^j$.
4. Build the numerical model associated with the jth scenario.

5. Construct a feature vector $\mathbf{X}^j$ using the antiresonant frequencies derived from the numerical model.
6. Add the pair of vectors $(\mathbf{X}^j, \mathbf{Y}^j)$ to the database, set $j = j + 1$ and go to step 3.

3.1. Feature vector

The jth feature vector $\mathbf{X}^j$ contains the experimental changes in the antiresonant frequencies with respect to the intact case:

$$\mathbf{X}^j = \left\{ \frac{\omega_{1,1}^D - \omega_{1,1}^U}{\omega_{1,1}^U}, \frac{\omega_{2,1}^D - \omega_{2,1}^U}{\omega_{2,1}^U}, \ldots, \frac{\omega_{n_1,1}^D - \omega_{n_1,1}^U}{\omega_{n_1,1}^U}, \ldots, \frac{\omega_{n_r,r}^D - \omega_{n_r,r}^U}{\omega_{n_r,r}^U} \right\}, \quad (11)$$

The superscripts D and U refer to damaged and undamaged, respectively, and $\omega_{i,r}$ is the ith antiresonant frequency of the rth Frequency Response Function (FRF). Experimental antiresonances are identified from transmissibility measurements using the algorithm presented in [39].

3.2. Observation vector

The jth observation vector $\mathbf{Y}^j$ contains damage indices represented by elemental stiffness reduction factors, defined as the ratio of the stiffness reduction to the initial stiffness. The stiffness matrix of the damaged structure, $\mathbf{K}_d$, is expressed as a sum of element matrices multiplied by reduction factors:

$$\mathbf{K}_d = \sum_{i=1}^{m} \left(1 - Y_i^j\right) \mathbf{K}_i, \quad (12)$$

where $\mathbf{K}_i$ is the stiffness matrix of the ith element. Thus, $Y_i^j = 0$ indicates that the ith element is undamaged, whereas $0 < Y_i^j < 1$ implies partial damage and $Y_i^j = 1$ complete damage.

3.3. Distribution of patterns

The distribution of patterns in the database plays a crucial role in the success of the algorithm. The relationship between antiresonant frequencies and different damage levels is not linear. Therefore, the algorithm might not be able to interpolate data. In this study, the patterns were generated by considering single damage scenarios with eight damage levels distributed as 0, 20, 40, 60, 80, 90, 95 and 99.9%.

4. Application cases

The results of the max-ent linear approximation algorithm are compared with those obtained by a multilayer feedforward neural network approach [14] and a model updating method based on parallel genetic algorithms [39]. The neural network was trained with the same database used for the max-ent linear approximation method, but polluted with 1.0% random noise to minimize false damage detection due to experimental noise [14]. The procedure to assess the experimental damage using the max-ent linear approximation is implemented as follows:

1. Perform an experimental test of the damaged structure and identify the antiresonant frequencies.
2. Construct the feature test point $\mathbf{X}$ using (11).
3. Read the feature vectors in the database.
4. Select parameter β_i in the Gaussian prior given in (7), so that k neighbours contribute to the solution.
5. Solve the system of nonlinear equations presented in (10).
6. Compute the weight functions from (8).

7. Read the observation vectors in the database and estimate the experimental damage from (3).

The next sub-sections present each application case and the results obtained by the three approaches.

4.1. Eight-DOF spring-mass system

The structure shown in Fig. 4 consists of an eight-DOF spring-mass system. Los Alamos National Laboratory (LANL) designed and constructed this system to study the effectiveness of various vibration-based damage identification techniques [50]. Eight translating masses connected by springs form the system. Each mass is a disc of aluminium with a diameter of 76.2 mm and a thickness of 25.4 mm. The masses slide on a highly polished steel rod and are fastened together with coil springs. The positions of the springs and masses are designated sequentially, with the first ones being closest to the shaker attachment.

In the undamaged configuration, all springs are identical and have a linear stiffness coefficient. Damage was simulated by replacing the fifth spring with another spring that has a lower stiffness (55% stiffness reduction). Acceleration was measured horizontally at each mass yielding eight measured DOFs. The structure was excited randomly by an electro-dynamic shaker. Twenty-eight antiresonant frequencies were identified from the transmissibility measurements.

The numerical model was built in `Matlab`® with springs and concentrated masses. The initial parameters were as follows:

- Mass 1: 559.3 g (This mass is greater than the others due to the hard-

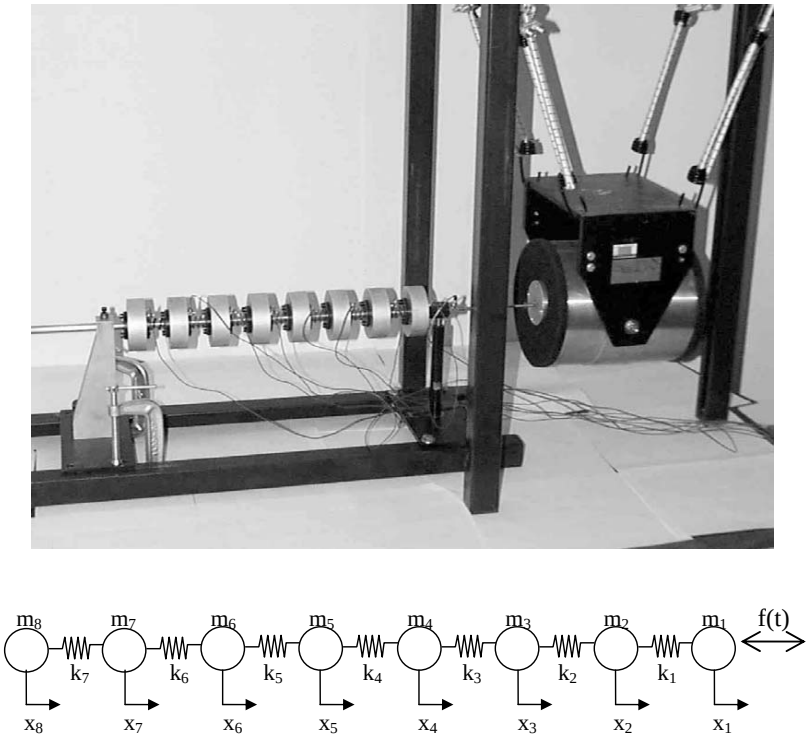

Figure 4: Experimental eight-degrees-of-freedom system.

ware required to attach the shaker)

- Masses 2 to 8: 419.4 g
- Spring constants: 56.7 kN/m

In the undamaged case, the maximum difference between the experimental and numerical antiresonances was 3.7%. The database samples were created using the seven springs as possible locations for damage, resulting in 56 patterns.

During the set-up of the damage identification algorithm, the only parameter that needs to be selected in the max-ent computation is γ for the

Gaussian prior. This parameter controls the radius of the weight functions associated with those feature vectors $\mathbf{X}^j$ that contribute to the approximation at the feature test vector $\mathbf{X}$. Therefore, it determines the number of neighbors to the test point. In addition, the weights associated with the active neighbors are determined up on their distances to the test point. The closer the distance, the larger the weight. Fig. 5 shows the damage assessment results using the values $\gamma = 1$, 100, 800 and 1600. An horizontal line indicates the actual stiffness reduction. In each case there are 57, 46, 6 and 2 neighbors contributing to the final solution, respectively. These results indicate that using a larger value of γ results in more accurate solutions. Nevertheless, if γ is too high there might not be enough neighbors to build the approximation.

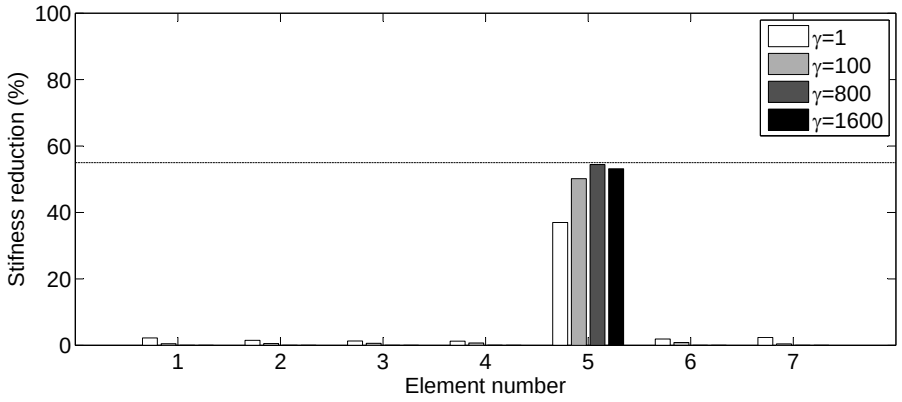

Figure 5: Damage identification results for the eight-degrees-of-freedom mass-spring system using different values for γ in the Gaussian prior.

Fig. 6 shows the results for the experimental damage case using $\gamma = 800$. The results are compared with those obtained using model updating and

neural networks methods. The three methods were able to correctly identify the experimental damage represented by a 55% stiffness reduction in element 5, although the neural network identifies a small false damage at element 2. In terms of time, the model updating approach required 206 seconds to yield a solution, the linear approximation required 0.2 seconds, whereas the neural network required only 0.09 seconds. It should be noted that linear approximation and neural network algorithms can reach a solution in less than a second, which can be considered real-time for structural damage assessment problems.

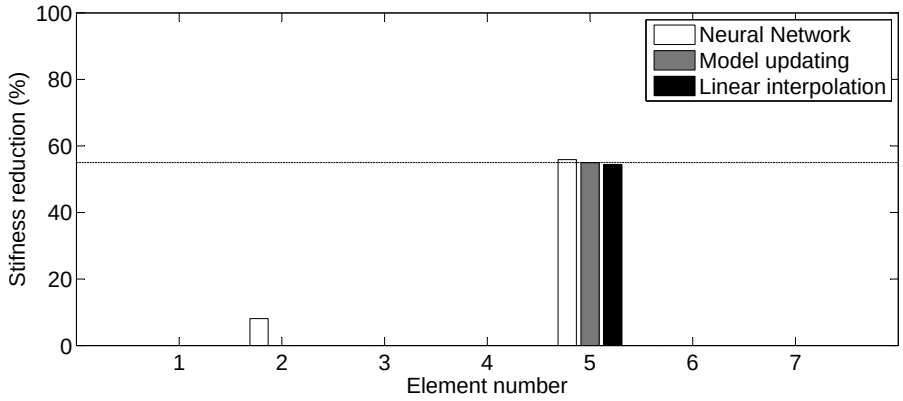

Figure 6: Identification of experimental damage in the eight DOF mass-spring system using two algorithms: linear approximation with maximum entropy and model updating with parallel genetic algorithms.

4.2. Experimental beam

In the second experimental case, the structure consisted of a steel beam with a rectangular cross-section. The beam measured 1 m in length and had a cross-sectional area of $25 \times 10\,\mathrm{mm}^2$. As shown in Fig. 7, soft springs suspend

the structure to simulate a "free-free" boundary condition. A shaker excites the beam at one end, and the response is measured by 11 accelerometers. Both the excitation force and the measured responses are in the horizontal direction. In this direction, antiresonant frequencies are more sensitive to the experimental damage. Thirty-six antiresonant frequencies were identified from the transmissibility measurements.

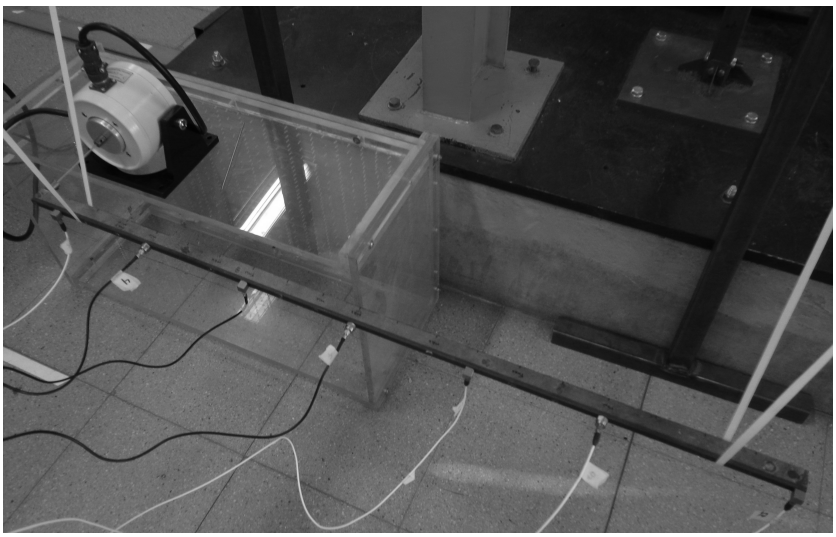

Figure 7: Experimental beam.

The numerical model was built in `Matlab`® with 2D beam elements. The model featured 20 beam elements and 40 degrees of freedom, as shown in Fig. 8. In the undamaged case, the maximum difference between the experimental and numerical antiresonances was 3.63%. Shadowed elements represent possible locations of damage, resulting in 18 damage locations and 144 patterns.

The structure was subjected to three different damage scenarios containing single cracks. Cracks were introduced into the structure by saw cuts, as

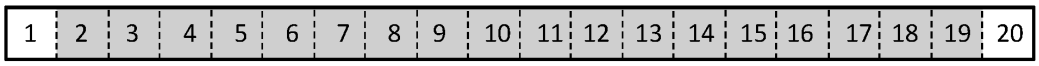

Figure 8: Numerical model of the beam and element numbering.

illustrated in Fig. 9. Table 1 summarizes the damage scenarios indicating the distance from the left-end to the cut, the corresponding element in the numerical model, and the cut length. In the first damage scenario the cut is in between elements 9 and 10.

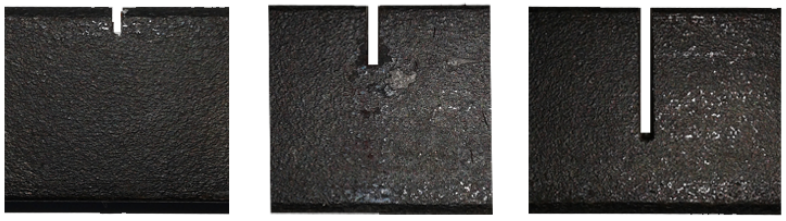

Figure 9: Saw cuts introduced into the beam.

Damage scenario	Distance from the left end (mm)	Element number	Saw cut length (mm)
1	450	9-10	3
2	685	14	7
3	810	17	15

Table 1: Damage scenarios introduced to the beam

The parameter γ in the Gaussian prior is selected so 6 neighbors contribute to the solution. Fig. 10 shows the results of the experimental damage identified by three approaches: neural network, model updating and linear

approximation. An arrow indicates the actual damage location. In the first damage scenario, the only approach that detected a damage in the actual location is the max-ent linear approximation, detecting 8% stiffness reduction in elements 9 and 10. In the second and third damage scenarios, damage is correctly located by the three approaches. Although with the neural network approach damage quantification is not accurate and a few false damages are detected.

In terms of time, the model updating approach requires approximately 900 seconds to assess the experimental damage, the linear approximation requires 0.3 seconds, whereas the neural network requires only 0.1 seconds.

4.3. Car Exhaust System

The structure consists of a car exhaust system as shown in Fig. 11. The dimensions are: length: 2.3 m, width: 0.45 m. The exhaust pipe has a diameter of 38 mm. The structure is suspended by soft springs and is excited randomly by an electrodynamic shaker. The response is captured by 16 accelerometers. The test is performed in a frequency range of $0 - 512$ Hz with a frequency resolution of 0.25 Hz.

The numerical model shown in Fig. 12 was built in `Matlab`® with $2D$ beam elements and concentrated inertias for the masses. The model has 47 beam and 5 inertia elements, with 144 degrees of freedom. Thirty-two antiresonances were identified from the transmissibility functions. All of them are used during the model updating process. The maximum difference between the experimental and numerical antiresonances after updating was 7.6%.

A single fatigue crack with three increasing levels of damage is introduced

to the structure. Fig. 13-a) shows the crack, which is located in element 31, close to the welded connection between elements 30 and 31 and covers around 60% of the pipe perimeter. The fatigue test is done again twice to grow the crack. Fig. 13-b) shows the second damage level; here the structure has already failed due to unstable crack propagation. The open crack covers around 70% of the perimeter. The last damage level is shown in Fig. 13-c). The crack covers around 85% of the perimeter.

Elements 18 to 47 are considered possible locations of damage, giving 30 damage locations and 240 patterns.

The parameter γ in the Gaussian prior is selected so six neighbors patterns contribute to the solution. Fig. 14 shows the results of the experimental damage identified by the three approaches: neural network, model updating and linear approximation. An arrow indicates the actual damage location. In the three damage scenarios, the damage is correctly identified by the linear approximation and the model updating approaches. Though, in the first case the damage detected by the linear approximation approach is closer to the actual location. On the other hand, the neural network technique, instead of detecting one large damage, it detects two to three medium damages at locations near the actual one.

In terms of time, the model updating approach requires approximately 1800 seconds to assess the experimental damage in each case, the linear approximation approach requires 0.7 seconds, whereas the neural network requires only 0.2 seconds.

5. Conclusions

This article presented a new supervised learning algorithm for real-time damage assessment that uses a linear approximation method in conjunction with antiresonant frequencies that are identified from transmissibility functions. The linear approximation is handled by a statistical inference model based on the maximum-entropy principle. The performance of the proposed methodology was validated by considering three experimental structures: an eight-DOF mass-spring system, a beam, and an exhaust system of a car.

To demonstrate the potential of the proposed algorithm over existing ones, the obtained results are compared with those of a model updating method based on parallel genetic algorithms and a multilayer feedforward neural network approach. The results show that the neural network was the fastest in assessing damage, but quantification was not accurate. The model updating, on the other hand, provides accurate results, but it requires between 3 to 30 minutes to assess damage. The max-ent linear approximation combines the best of both; it provides a fast and accurate damage assessment. In the three structures, the max-ent linear approximation was successful in assessing the experimental damage. The detected damage closely corresponds to the experimental damage in all cases, obtaining results very similar to those of a model updating approach in a processing time equivalent to neural networks. Hence, the proposed algorithm provides the possibility of continuously monitoring the state of a structure.

The three structures used to validate the damage assessment algorithm are unidimensional in nature. Although the exhaust system is a 2D structure, it behaves similar to an unidimensional structure. Thus, more research is

needed to test the performance of the proposed algorithm with 2D and 3D structures.

The linear max-ent approximation method, as presented, is able to accurately assess single damage scenarios. Further research is needed to adapt this algorithm to cases with multiple damage scenarios.

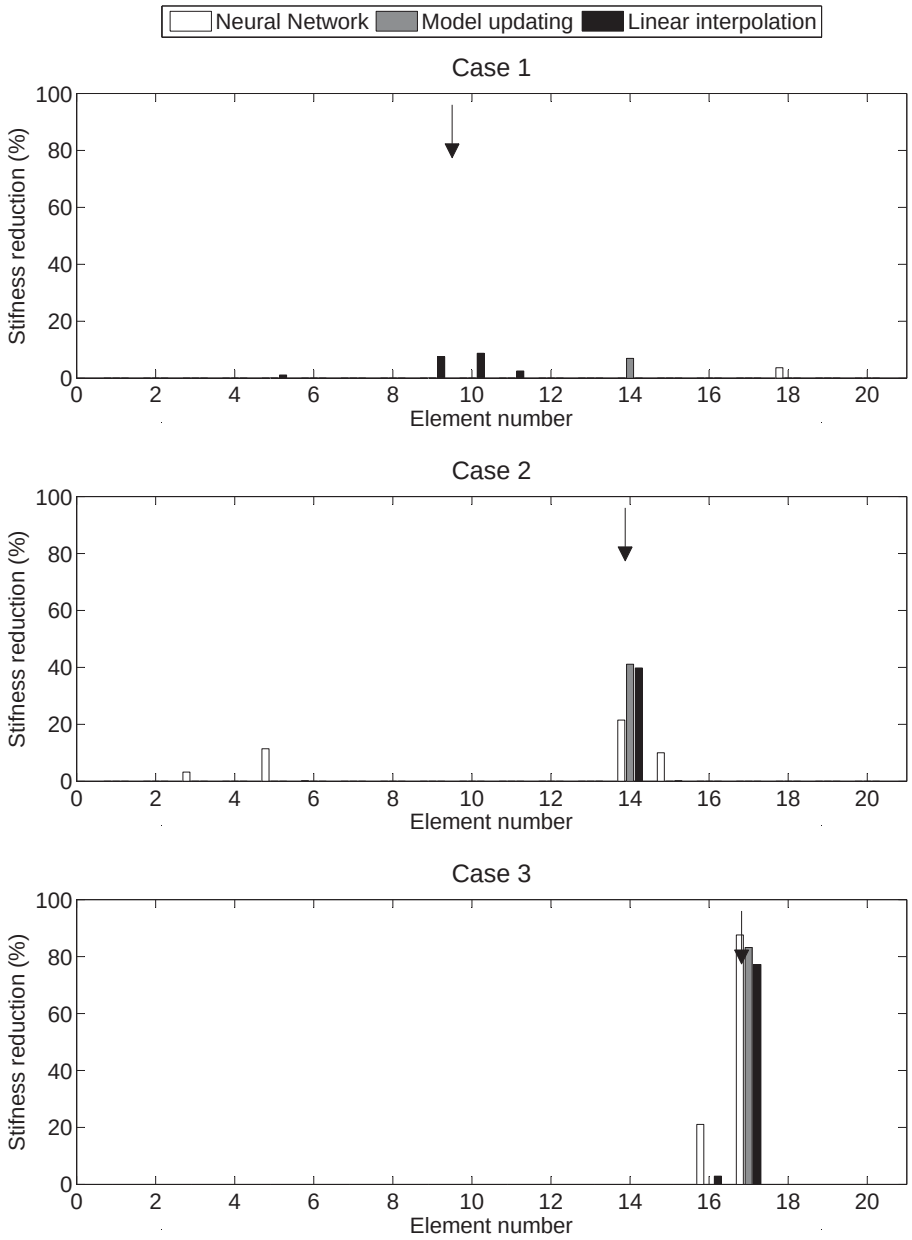

Figure 10: Identification of experimental damage in the beam using two algorithms: linear approximation with maximum entropy and model updating with parallel genetic algorithms.

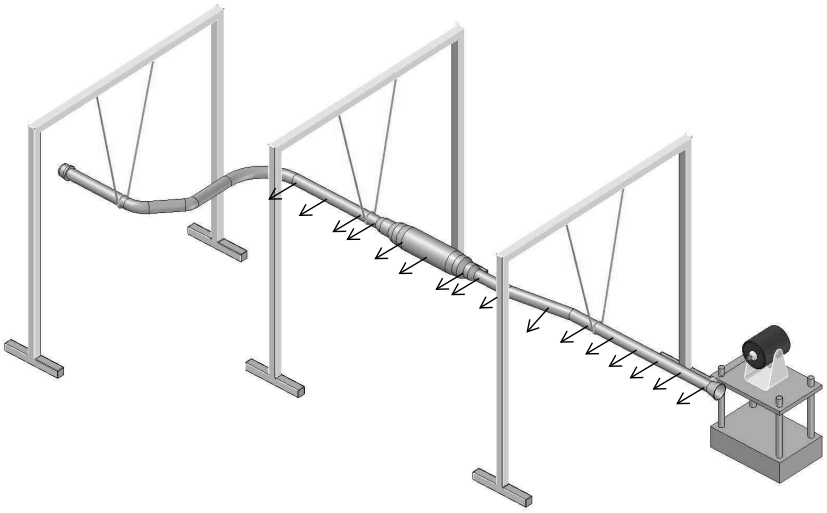

Figure 11: Experimental set-up of the car exhaust system.

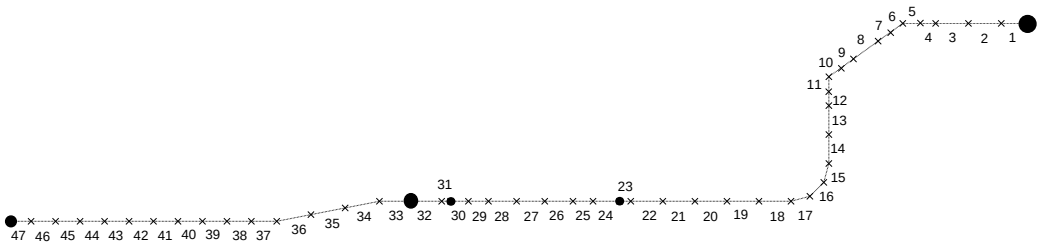

Figure 12: Finite element model and element numbering of the car exhaust system.

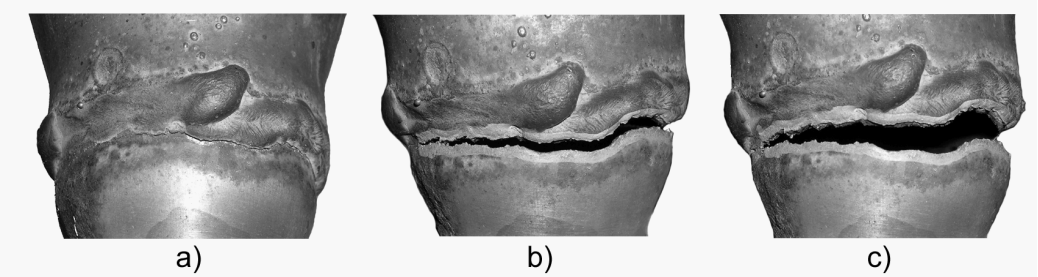

Figure 13: Three levels of damage introduced to the car exhaust system.

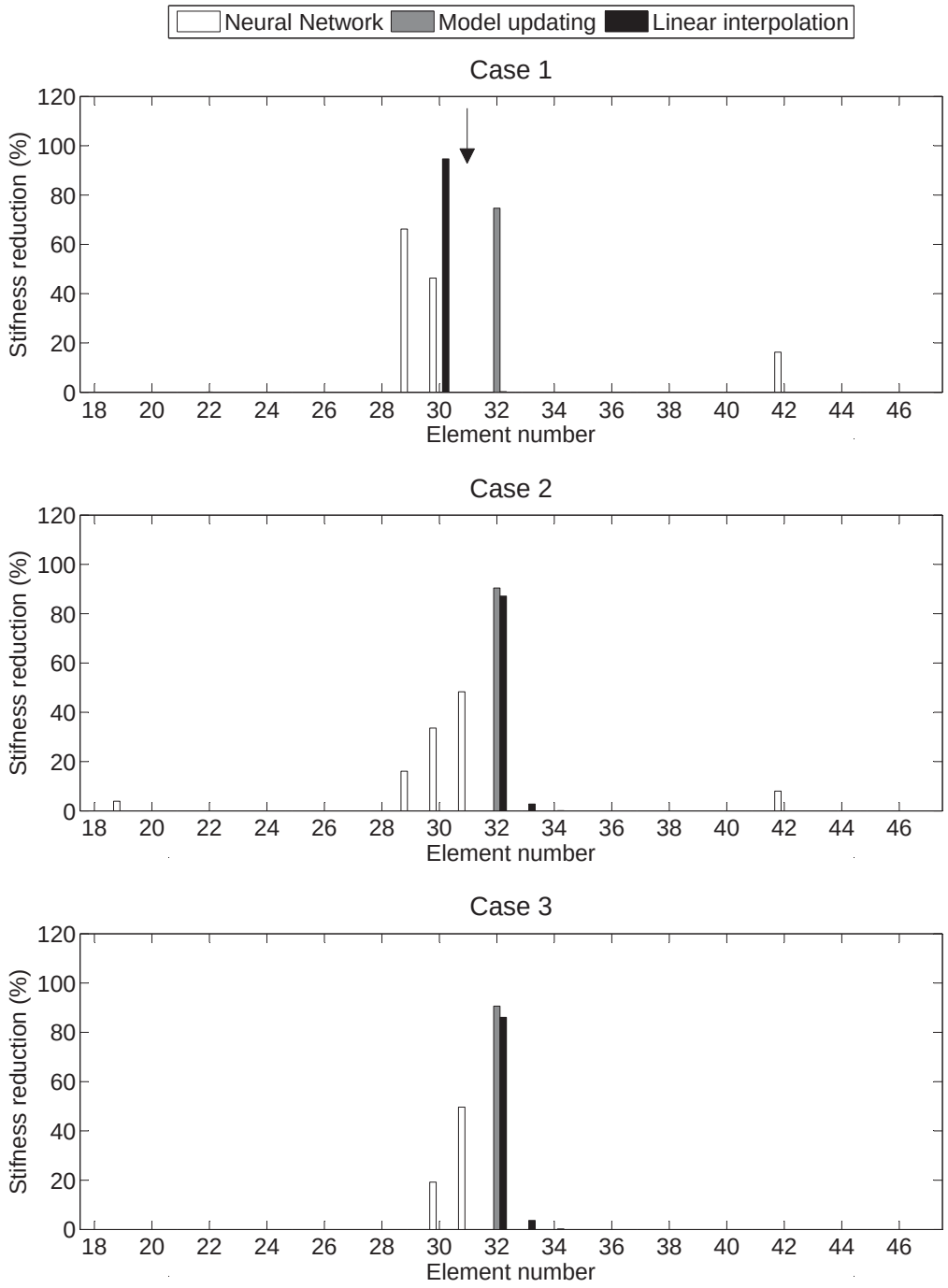

Figure 14: Identification of experimental damage in the car exhaust system using two algorithms: linear approximation with maximum entropy and model updating with parallel genetic algorithms.

Acknowledgments

The authors acknowledge the partial financial support of the Chilean National Fund for Scientific and Technological Development (Fondecyt) under Grants No. 11110389 and 11110046.

References

[1] E. Carden, P. Fanning, Vibration based condition monitoring: A review, Structural Health Monitoring 3 (4) (2004) 355–377.

[2] Y. Yan, L. Cheng, Z. Wu, L. Yam, Development in vibration-based structural damage detection technique, Mechanical Systems and Signal Processing 21 (5) (2007) 2198–2211.

[3] C. Farrar, N. Lieven, Damage prognosis: the future of structural health monitoring, Philosophical Transactions of the Royal Society A: Mathematical, Physical and Engineering Sciences 365 (1851) (2007) 623–632.

[4] V. Meruane, W. Heylen, Damage detection with parallel genetic algorithms and operational modes, Structural Health Monitoring 9 (6) (2010) 481–496.

[5] V. Meruane, W. Heylen, An hybrid real genetic algorithm to detect structural damage using modal properties, Mechanical Systems and Signal Processing 25 (2011) 1559–1573.

[6] R. Perera, R. Torres, Structural damage detection via modal data with genetic algorithms, Journal of Structural Engineering 132 (9) (2006) 1491–1501.

[7] B. Kouchmeshky, W. Aquino, J. Bongard, H. Lipson, Co-evolutionary algorithm for structural damage identification using minimal physical testing, International Journal for Numerical Methods in Engineering 69 (5) (2007) 1085–1107.

[8] A. Teughels, G. De Roeck, J. Suykens, Global optimization by coupled local minimizers and its application to FE model updating, Computers & Structures 81 (24-25) (2003) 2337–2351.

[9] C. C. Ciang, J.-R. Lee, H.-J. Bang, Structural health monitoring for a wind turbine system: a review of damage detection methods, Measurement Science and Technology 19 (12) (2008) 122001(20pp).

[10] M. Markou, S. Singh, Novelty detection: a review-part 1: statistical approaches, Signal Processing 83 (12) (2003) 2481–2497.

[11] C. Gonzalez-Perez, J. Valdes-Gonzalez, Identification of structural damage in a vehicular bridge using artificial neural networks, Structural Health Monitoring 10 (1) (2011) 33–48.

[12] B. Sahoo, D. Maity, Damage assessment of structures using hybrid neuro-genetic algorithm, Applied Soft Computing 7 (1) (2007) 89–104.

[13] S. Arangio, J. Beck, Bayesian neural networks for bridge integrity assessment, Structural Control and Health Monitoring 19 (1) (2012) 3–21.

[14] V. Meruane, J. Mahu, Real-time structural damage assessment using artificial neural networks and anti-resonant frequencies, Shock and Vibration 2014 (2014) 653279(14pp).

[15] M. R. Gupta, An information theory approach to supervised learning, Ph.D. thesis, Stanford University (2003).

[16] M. R. Gupta, R. M. Gray, R. A. Olshen, Nonparametric supervised learning by linear interpolation with maximum entropy, Pattern Analysis and Machine Intelligence, IEEE Transactions on 28 (5) (2006) 766–781.

[17] E. T. Jaynes, Information theory and statistical mechanics, Physical Review 106 (4) (1957) 620–630.

[18] A. N. Erkan, Semi-supervised learning via generalized maximum entropy, Ph.D. thesis, New York University (2010).

[19] A. Ortiz, M. A. Puso, N. Sukumar, Maximum-entropy meshfree method for compressible and near-incompressible elasticity, Computer Methods in Applied Mechanics and Engineering 199 (25–28) (2010) 1859–1871.

[20] A. Ortiz, M. Puso, N. Sukumar, Maximum-entropy meshfree method for incompressible media problems, Finite Elements in Analysis and Design 47 (6) (2011) 572–585.

[21] A. Kyprianou, C. Mares, C. D. Charalambous, J. E. Mottershead, Minimum relative entropy criterion for damage detection and location, Key Engineering Materials 347 (2007) 421–426.

[22] C. Mares, A. Kyprianou, Minimum relative entropy criterion for damage detection and location, in: Proceedings of the International Modal Analysis Conferece, IMAC XXVII, Orlando, Florida, USA, 2009.

[23] S. Hakim, H. A. Razak, Frequency response function-based structural damage identification using artificial neural networks-a review, Research Journal of Applied Sciences, Engineering and Technology 7 (9) (2014) 1750–1764.

[24] S. Chesné, A. Deraemaeker, Damage localization using transmissibility functions: a critical review, Mechanical systems and signal processing 38 (2) (2013) 569–584.

[25] K. Worden, Structural fault detection using a novelty measure, Journal of Sound and vibration 201 (1) (1997) 85–101.

[26] K. Worden, G. Manson, The application of machine learning to structural health monitoring, Philosophical Transactions of the Royal Society A: Mathematical, Physical and Engineering Sciences 365 (1851) (2007) 515–537.

[27] K. Worden, L. Cheung, J. Rongong, Damage detection in an aircraft component model, in: Proceedings of the International Modal Analysis Conference, IMAC XIX, 2001, pp. 1234–1241.

[28] K. Worden, G. Manson, D. Allman, Experimental validation of a structural health monitoring methodology: Part i. novelty detection on a laboratory structure, Journal of Sound and Vibration 259 (2) (2003) 323–343.

[29] G. Manson, K. Worden, D. Allman, Experimental validation of a structural health monitoring methodology: Part iii. damage location on an aircraft wing, Journal of Sound and Vibration 259 (2) (2003) 365–385.

[30] G. Manson, K. Worden, D. Allman, Experimental validation of a structural health monitoring methodology: Part ii. novelty detection on a gnat aircraft, Journal of Sound and Vibration 259 (2) (2003) 345–363.

[31] S. Pierce, K. Worden, G. Manson, A novel information-gap technique to assess reliability of neural network-based damage detection, Journal of Sound and Vibration 293 (1) (2006) 96–111.

[32] H. Zhang, M. Schulz, A. Naser, F. Ferguson, P. Pai, Structural health monitoring using transmittance functions, Mechanical Systems and Signal Processing 13 (5) (1999) 765–787.

[33] T. Johnson, D. Adams, Transmissibility as a differential indicator of structural damage, Journal of Vibration and Acoustics 124 (4) (2002) 634–641.

[34] T. J. Johnson, R. L. Brown, D. E. Adams, M. Schiefer, Distributed structural health monitoring with a smart sensor array, Mechanical Systems and Signal Processing 18 (3) (2004) 555–572.

[35] N. Maia, J. Silva, A. Ribeiro, The transmissibility concept in multi-degree-of-freedom systems, Mechanical Systems and Signal Processing 15 (1) (2001) 129–137.

[36] R. Sampaio, N. Maia, A. Ribeiro, J. Silva, Transmissibility techniques for damage detection, in: Proceedings of the International Modal Analysis Conference, Vol. 2, 2001, pp. 1524–1527.

[37] N. M. Maia, R. A. Almeida, A. P. Urgueira, R. P. Sampaio, Damage

detection and quantification using transmissibility, Mechanical Systems and Signal Processing 25 (7) (2011) 2475–2483.

[38] G. Steenackers, C. Devriendt, P. Guillaume, On the use of transmissibility measurements for finite element model updating, Journal of Sound and Vibration 303 (3-5) (2007) 707–722.

[39] V. Meruane, Model updating using antiresonant frequencies identified from transmissibility functions, Journal of Sound and Vibration 332 (4) (2013) 807–820.

[40] C. Devriendt, P. Guillaume, Identification of modal parameters from transmissibility measurements, Journal of Sound and Vibration 314 (1-2) (2008) 343–356.

[41] C. Devriendt, G. Steenackers, G. De Sitter, P. Guillaume, From operating deflection shapes towards mode shapes using transmissibility measurements, Mechanical Systems and Signal Processing 24 (3) (2010) 665–677.

[42] C. Devriendt, W. Weijtjens, G. De Sitter, P. Guillaume, Combining multiple single-reference transmissibility functions in a unique matrix formulation for operational modal analysis, Mechanical Systems and Signal Processing 40 (1) (2013) 278–287.

[43] K. Hormann, N. Sukumar, Maximum entropy coordinates for arbitrary polytopes, Computer Graphics Forum 27 (2008) 1513–1520.

[44] C. E. Shannon, A mathematical theory of communication, The Bell Systems Technical Journal 27 (1948) 379–423.

[45] N. Sukumar, R. W. Wright, Overview and construction of meshfree basis functions: from moving least squares to entropy approximants, International Journal for Numerical Methods in Engineering 70 (2) (2007) 181–205.

[46] S. Kullback, Information Theory and Statistics, Wiley, New York, NY, 1959.

[47] J. E. Shore, R. W. Johnson, Axiomatic derivation of the principle of maximum entropy and the principle of minimum cross-entropy, IEEE Transactions on Information Theory 26 (1) (1980) 26–36.

[48] M. Arroyo, M. Ortiz, Local maximum-entropy approximation schemes: a seamless bridge between finite elements and meshfree methods, International Journal for Numerical Methods in Engineering 65 (13) (2006) 2167–2202.

[49] J. J. Lee, J. W. Lee, J. H. Yi, C. B. Yun, H. Y. Jung, Neural networks-based damage detection for bridges considering errors in baseline finite element models, Journal of Sound and Vibration 280 (3) (2005) 555–578.

[50] T. Duffey, S. Doebling, C. Farrar, W. Baker, W. Rhee, S. Doebling, Vibration-based damage identification in structures exhibiting axial and torsional response, Transactions of the ASME-L-Journal of Vibration and Acoustics 123 (1) (2001) 84–91.